Water Science & Technology

Water Science & Technology Vol 89 No 2, 333 doi: 10.2166/wst.2023.418

Application of a hybrid-fruit-peel (HFP) coagulant in low carbon source wastewater treatment as an external carbon source

Ying Fu[a,*], Qinghe Yue[a,b], Shuyuan Luo[a] and Xi Tian[c]

[a] School of Civil Engineering and Architecture, University of Jinan, 336, West Rode of Nan Xinzhuang, Jinan 250022, China
[b] First Construction Co., LTD., China Construction Eight Engineering Division Corp., LTD, 89, South Rode of Gongye, Jinan 250014, China
[c] Shuifa Technology Group Co., Ltd., 30, Huayang Rode, Shandong, Jinan 250199, China
*Corresponding author. E-mail: cea_fuy@ujn.edu.cn

ABSTRACT

The application of a hybrid-fruit-peel (HFP) coagulant used as an external carbon source (ECS) in both simulated water and real sewage having a low carbon source treated with sequencing batch reactor (SBR) was studied, compared with that of sodium acetate (NaAc). The impact of HFP on sludge properties (such as extracellular polymer substance (EPS), dehydrogenase activity (DHA), charged property, size, microscopic images and bacteria phase) was characterized. The results showed that as an ECS, HFP basically gave similar nitrogen removal to NaAc and also gave a similar developing trend of both dissolved oxygen (DO) and pH. HFP promoted more proliferation of microorganisms and posed higher levels of protein (PN) and polysaccharide (PS) than NaAc, but gave slightly lower DHA than NaAc. After HFP was added as an ECS, the types and quantities of microorganisms increased significantly, the effluent qualities were improved and the sludge size and extensibility became larger, which was conducive to direct contact and remove pollutants. HFP played a similar role to NaAc as ECS and can be used as a quality and slow-releasing ECS for low carbon source wastewaters.

Key words: external carbon source, hybrid-fruit-peel (HFP) coagulant, low carbon source wastewater, sequencing batch reactor (SBR), sludge properties

HIGHLIGHTS

- Application of HFP coagulant as an external carbon source (ECS) for low C/N wastewater was studied and gave a similar effect to NaAc.
- HFP can be used as a quality and slow-releasing ECS for low C/N wastewater.
- HFP produced sludge has a larger size and better extensibility.
- HFP promoted more proliferation of microorganisms and gave better effluent qualities.

GRAPHICAL ABSTRACT

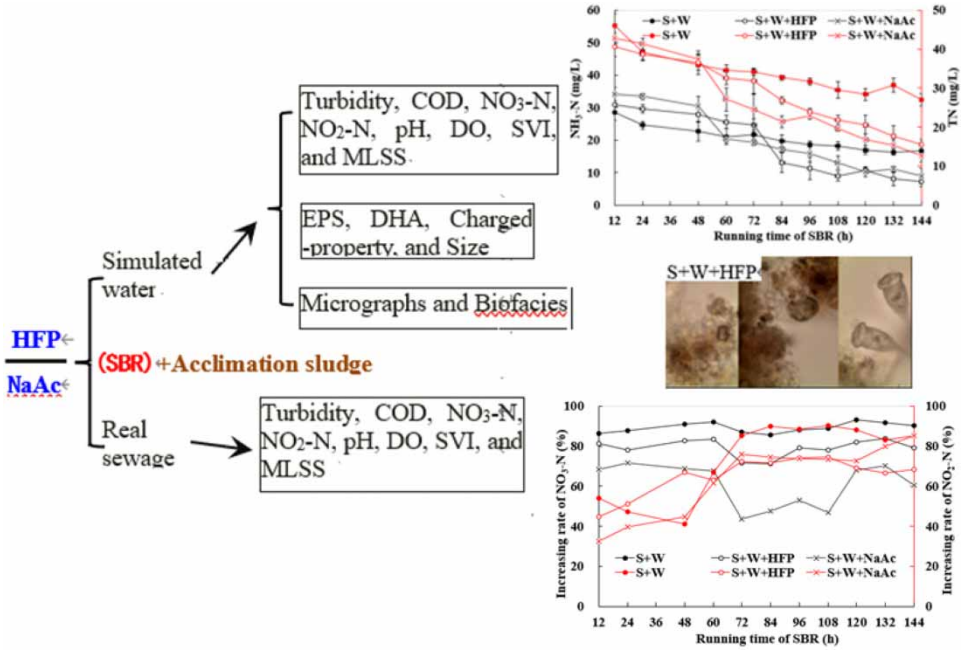

1. INTRODUCTION

With the largely increasing population growth, urbanization and industrialization, freshwater pollution and the shortage are becoming more and more serious in China. Wastewater reuse probably becomes one of the final important methods to solve the problems. With the increasing improvement of people's living standards, water consumption in China continually rises, leading to a decrease in organic matter level and an increase in chemicals containing nitrogen (N) in sewages (Zhang *et al.* 2022; Li *et al.* 2023). In addition, the specific layout of sewage pipes in China led to a continuous reduction of the ratio of chemical oxygen demand (COD) to total nitrogen (TN) (C/N) in urban sewages (Yu *et al.* 2019a, 2019b; Sun 2020). China's inherent eating habits also exacerbated this phenomenon. Presently, anaerobic–anoxic/Oxic (A^2/O), sequencing batch reactor (SBR), oxidation ditch and other processes are generally used in urban sewage treatment plants in China, in which nitrogen removal mainly depends on nitrogen nitrification and denitrification technologies. Generally, the denitrifying bacteria can be well proliferated when the C/N ratio in the influent is greater than 4. However, the organic matter level (as COD) in municipal sewage in most cities in China was less than 200 mg/L and the C/N ratio was around 3.5 or even lower (Awual 2019; Yu *et al.* 2019a, 2019b; Zhang *et al.* 2021; Bi *et al.* 2022; Feng *et al.* 2023). How to remove N efficiently from sewage is quite crucial for wastewater treatment because N discharge has many adverse effects on the environment, especially on eutrophication caused by excessive discharge of N and phosphorus (P). Currently, optimizing of intake pattern (Gu *et al.* 2019; Sun *et al.* 2020), some new processes (such as simultaneous nitrification denitrification (SND) and anaerobic ammonium oxidation (ANAMMOX)) (Shalini & Joseph 2018; Wang *et al.* 2019; Huang & Lee 2020; Ma *et al.* 2020; Chang *et al.* 2021; Li *et al.* 2021) and application of external carbon sources (ECS) are widely used in removing N from wastewater, in which the application of ECS has been extensively used in China (Hang *et al.* 2016; Xiong *et al.* 2020; Fu *et al.* 2023) in recent years.

The study on ECS is still one of the focuses in wastewater treatment with low carbon sources in influent in China, in which ECS mainly includes traditional type (having relatively large production) which generally consists of organic substances with lower molecular, such as acids, alcohols and carbohydrates (Cherchi *et al.* 2009; Fu *et al.* 2023) and new type which usually are solid, liquid and gas having larger molecular weight than the traditional type (Jiang *et al.* 2018; Xiong *et al.* 2019; Hu *et al.* 2020; Narancic *et al.* 2020; Qi *et al.* 2020; Mahmoud *et al.* 2022). Presently, more relevant research has been conducted on solid new type ECS (for instance, on agricultural and forestry wastes (AFWs)) (Jiang *et al.* 2018; Hu *et al.* 2019; Zhong *et al.* 2019; Zhou *et al.* 2019; Zeeshan *et al.* 2020; Fu *et al.* 2023), in which direct application of single function of AFWs as ECS has

been widely studied (Torresi *et al.* 2017; Pelaz *et al.* 2018; Qi *et al.* 2020; Zhao *et al.* 2020; Fu *et al.* 2023), but the studies of simultaneous multi-function of AFWs on lower carbon sources wastewater treatment was rarely focused.

Recently, the AFWs used to make coagulants and absorbents mainly include the peel of bananas, oranges, grapefruit, etc. (Hameed *et al.* 2008; Fu *et al.* 2019; Fu & Meng 2021; Kim 2022). These fruit peels basically consist of cellulose, pectin, hemicellulose, lignin, etc.; moreover, they have many active functional groups (hydroxyl and carboxyl) that are easily combined with pollutants through adsorption and coagulation action. Lots of fruit peels have entered into the environment as wastes, in which the organic components have simultaneously been discarded.

This work was about the application of an HFP coagulant (Fu *et al.* 2019; Fu & Meng 2021) as an ECS in treating lower C/N wastewater with SBR, in which the HFP has been successfully developed from the peels (one of AFWs containing a large amount of organic carbon) of both banana and orange by the authors. Sodium acetate (NaAc) was used as a compared ECS because NaAc is an extensively application ECS (Fu *et al.* 2022) for lower carbon wastewater in China.

This work aims at utilizing the both functions of coagulation and ECS of a new coagulant in treating lower C/N wastewater (Fu *et al.* 2023), significantly reducing water treatment cost and also realizing a closed cycle of the carbon source chain. This work tries to explore an important development direction for carbon sources in low C/N wastewater treatment in the future.

2. MATERIALS AND METHODS

2.1. Preparation of HFP

Some fresh peels of banana and orange (planted in China) of about 3 cm in length were firstly dried for 2 days at room temperature to make the dry peels and then were continuously dried at 70 °C for 24 h with GZX-9140MBE Electric Heat Forced Air Drying Oven (Shanghai Boxun, China), respectively (Fu *et al.* 2019; Fu & Meng 2021). The two kinds of dry peel were broken up by CS-700 High Speed Multi-function Pulverizer (COSUAI/Chaoshuai, Zhejiang, China) to prepare the banana and orange peel powders with around 40 mm diameter, respectively.

The banana and orange peel powders were mixed in ratios of 1–3 to prepare 125 g mixed powder, then 5 L sodium hydroxide solution (0.04 mol/L, industrial grade, Tianjin, China) was added to the mixed powder at room temperature and under medium stirring for 2–3 min and was continuously heated at 60 °C for 10 min to obtain a solid–liquid mixture (Fu *et al.* 2019, 2021). The solid–liquid mixture was filtrated with a qualitative filter paper (Tianjin, China) to obtain HFP coagulant with the following properties: pH = 10.4, density = 1.102×10^3 kg/m, w(Saccharides) = 70.3%, w(Mixed powder) = 25 g/L, TOC = 4.5 g/L, BOD5/COD (aeration 4 h) = 0.67–0.76 and C/N (aeration 4 h) = 39.8–39.3 (Lu 2017; Yue 2022), respectively. HFP gives more stable characteristics of storage, coagulation and ECS performance (Lu 2017; Jian 2019; Yue 2022). HFP was sealed with adhesive tape and stored at 5 °C before usage.

2.2. Test water samples

A simulated water and real sewage were used as the test water samples with low carbon source having C/N from 3.52/1 to 5.37/1. The simulated water (24 L) contains $C_6H_{12}O_6$ (4.8–12 g), NH_4Cl (4.1 g), KH_2PO_4 (1.055 g), $MgSO_4{\cdot}7H_2O$ (1.44 g), $CaCl_2$ (0.48 g) and soil leaching solution (30 mL) prepared from 10 g soil which was derived from the campus at University of Jinan. The real sewage was from the hydrolytic tank of the wastewater plant of the University of Jinan. The qualities of the above two test water samples are summarized in Table 1.

2.3. Raw sludge and acclimation process

The raw sludge originated from the Second Plant of Everbright Water Co. Ltd (Jinan, China) using anaerobic–anoxic–oxic (A^2O) process (Fu *et al.* 2023). The acclimation water sample for the raw sludge was the simulated water in Table 1, and

Table 1 | Qualities of test water samples

	Parameters						
Test water samples	**Turbidity (NTU)**	**Color (AU)**	**Temperature (°C)**	**pH**	**COD (mg/L)**	**[a]NH_3-N (mg/L)**	**[b]TN (mg/L)**
Simulated water	1.83–2.12	0.011–0.015	26–26.6	7.4–8.1	198.2–208.7	51–56.2	51.2–57.7
Real sewage	44.3–58	0.205–0.28	26.5–26.7	7.4–8.1	268–306	57–66	66–72

[a]Ammonia-nitrogen.
[b]Total nitrogen.

the acclimation temperature was maintained at 25 + 5 °C and pH at 7–8, which included three phases: initial phase of 1 day; stable phase of 7 days including four stages of aerobic, anoxic, settling and drawing; adjustment phase of 22–25 days. The C/TN of the influent was adjusted by decreasing COD to get the following target: the C/TN of the influent was reduced to 4/1 when the COD was reduced to 200 mg/L. Then COD, NH_3-N and mixed liquor suspended solids (MLSS) in both influent and effluent were analyzed, respectively. COD and NH_3-N were determined by the Potassium dichromate method and Nessler's reagent colorimetric method (UV-5800 UV spectrophotometer, Shanghai Yuanxi), respectively. MLSS was determined by the gravimetric method. The properties of the acclimation sludge were as follows: NH_3-N was 19.5 mg/L, COD was 25.6 mg/L, SV_{30} was 34 mg/L, MLSS was 9,427 mg/L, temperature was 25.7 °C and pH was 7.5, respectively.

2.4. Experiment on the influence of HFP addition on wastewater treatment with SBR

The SBR system includes three traditional SBR (diameter = 15 cm and height = 26 cm for each SBR) (Barros *et al.* 2021; Tao *et al.* 2022; Fu *et al.* 2023) (Figure 1) having an effective volume of 1.8 L for each SBR was applied as bioreactors and the simulated water and real sewage in Table 1 were used as the test water samples.

The three SBRs were operated under the same conditions, in which the intermittent aeration and intermittent inflow/effluent were utilized during the whole process, in which their automatic operation was controlled by relay controls. The inflow and effluent were controlled by peristaltic pumps and solenoid valves, respectively. The temperature of SBR was kept at about 25 °C.

In each SBR, the total operation time of 144 h included 36 cycles with one cycle of 4 h which consisted of filling, reaction, settling and drawing with their time of 3, 175, 55 and 3 min, respectively. The filling volume was 0.6 L (i.e. the hydraulic retention time (HRT) was 12 h), the same as that for the drawing volume. The dosages of both HFP and NaAc were 0.181 g/L, and the initial MLSS of the sludge was 3,000 mg/L. The effluent was taken out every 12 h for the analysis of the following parameters: turbidity, COD, NH_3-N and TN, NO_3-N and NO_2-N, pH and dissolved oxygen (DO) which were determined with 2100AN Turbidimeter (Hach, USA), potassium dichromate method, Nessler's reagent colorimetric method and alkaline potassium persiflage digestion-UV spectrophotometric method (UV-5800 UV spectrophotometer, Shanghai Yuanli), UV spectrophotometry (220 and 275 nm) and N-(1-naphthalene)-ethylenediamine spectrophotometry (540 nm), S210-S pH meter (Mettler-Toledo, Switzerland) and 310D-01 table type DO meter (Visser Instruments Inc., USA), respectively. The surplus sludge was taken out every 12 h for the measurement of SV_{30} and MLSS with the measuring cylinder method and gravimetric method, respectively. The sludge volume index (SVI) was the ratio of SV_{30} divided by MLSS.

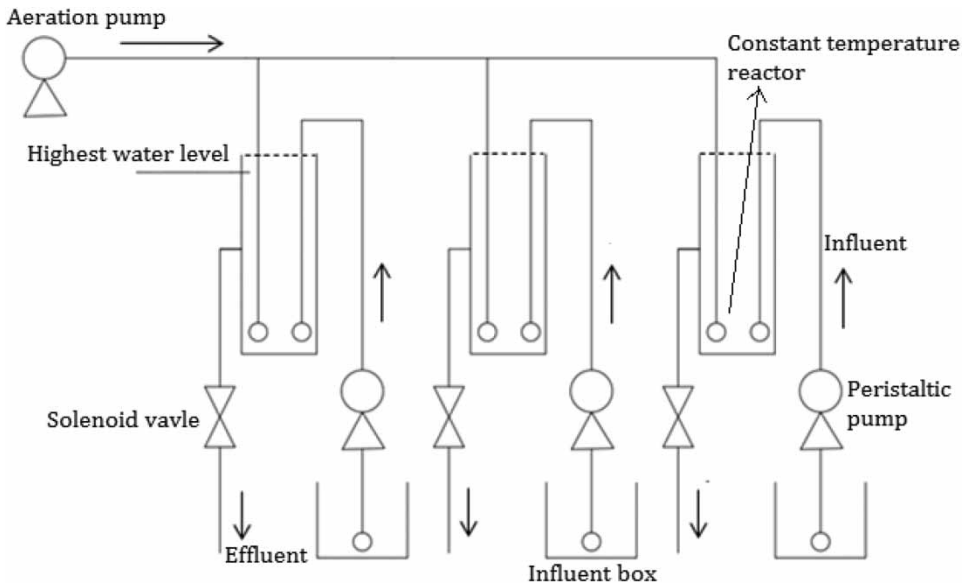

Figure 1 | Sequencing batch reactor (SBR) system device and process flow chart.

Three runs were performed for the simulated water, and the results represented the averages of the runs. Only one run was conducted for the real sewage, but turbidity and COD, pH and DO were measured three times in this run, so the results represented the averages of the measurements.

2.5. Experiment on influence of HFP addition on properties of surplus sludge with SBR

2.5.1. Extracellular polymer substance and DHA, charged property and size

The composition of the simulated water was relatively simple, so the extracellular polymer substance (EPS), DHA, charged property and size of the sludge from the simulated water treated were analyzed.

(1) EPS and DHA

At the end of SBR running, 100 mL surplus sludge was taken out and then precipitated for 30 min to obtain the precipitate which then was rinsed three times to gain the clean precipitate for measuring DHA and EPS. EPS includes soluble EPS (S-EPS) and bound EPS (B-EPS), in which B-EPS consists of loosely-bound EPS (LB-EPS) and tightly bound EPS (TB-EPS). EPS was the sum of protein (PN) and polysaccharide (PS), in which PN was the sum of soluble protein (S-PN) and loosely-bound protein (LB-PN) and tightly bound (TB-PN), and PS was the sum of soluble polysaccharide (S-PS) and loosely-bound polysaccharide (LB-PS) and tightly bound polysaccharide (TB-PS), respectively. DHA, PN and PS were measured with 2,3,5-triphenyl tetrazolium chloride (TTC)-reduction method (at wavelength 485 nm), and with Coomassie brilliant blue colorimetric method (at wavelength 595 nm) and anthrone-sulfuric acid method (at wavelength 620 nm) with UV-5800 Ultraviolet spectrophotometer (Shanghai, China), respectively.

EPS was determined as follows. Some pure water was added to half of the clean precipitate to get a 50 mL mixture which was then centrifuged at 4,000 r/min for 10 min; the analysis result of the supernatant was S-PN and S-PS; the residual precipitate A was obtained at the same time. Some pure water was added to the residual precipitate A to get a 50 mL mixture which was heated at 60 °C for 5 min, and then centrifuged at 12,000 r/min for 15 min; the analysis result of the supernatant was LB-PN and LB-PS; the residual precipitate B was obtained simultaneously. Some pure water was added to the residual precipitate B to get a 50 mL mixture which was also heated at 60 °C for 30 min and was then centrifuged at 12,000 r/min for 15 min; the analysis result of the supernatant was TB-PN and TB-PS.

(2) Charged property and size

The Zeta potential of the effluent: at the end of SBR running in Section 2.4, 100 mL effluent was taken out for the measurement of Zeta potential with Zetasizer Nano particle size potentiometer (Malvern, UK).

The Zeta potential of the sludge: a certain amount of clean precipitate in (1) in Section 2.5.1 was taken out and mixed with some pure water, and then was centrifuged under 12,000 r/min at 4 °C for 15 min to get a supernatant, and the Zeta potential of the supernatant was then measured using the same method as the effluent.

Some surplus sludge in Section 2.4 was taken out for the measurement of particle size with a Mastersize 3000 laser particle size analyzer (Shanghai Sibaiji, China).

Three runs were performed in this test, and the results represented the averages of the tests.

2.5.2. Micrographs

The surplus sludge in the real wastewater (Table 1) after SBR running 0, 3 and 6 days in Section 2.4 was taken out and placed onto the surface of glass slides, and then was observed and photographed with OLYMPUS CX31 optical microscope (Beijing Cnrico Technology Co., Ltd, China).

3. RESULTS AND DISCUSSION

3.1. Application of HFP in treating two kinds of wastewaters

In the following sections, 'S + W', 'S + W + HFP' and 'S + W + NaAc' refer to 'Sludge + Water sample', 'Sludge + Water sample + HFP' and 'Sludge + Water sample + NaAc', respectively. Since this work was to study the ECS function of HFP coagulant in treating wastewaters having low carbon sources, the SS removal from the effluent was replaced by turbidity removal. The turbidity in this section refers to the residual turbidity (RT) in the supernatant. Figures 2 and 3 showed the comparison of the effluent qualities and sludge settling performance (SSP) when HFP and NaAc were used as the ECS in the simulated water (Figure 2) and real sewage (Figure 3) with the SBR process. The dosage was 0.181 g/L, HRT was 12 h

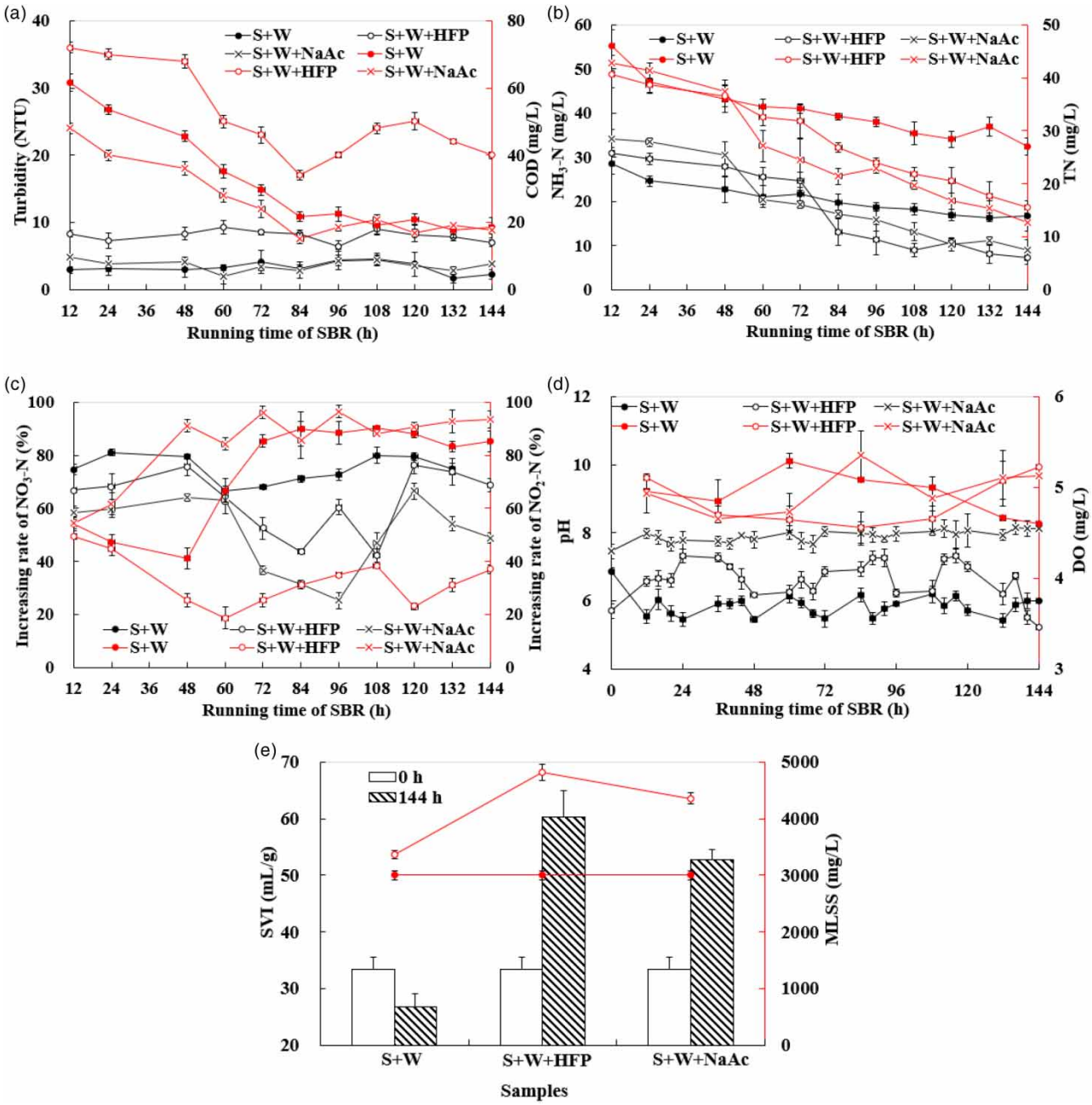

Figure 2 | Comparison of application effect of hybrid-fruit-peel coagulant (HFP) and sodium acetate (NaAc) in the simulated water with sequencing batch reactor (SBR) process between different test systems of 'Sludge + Water sample', 'Sludge + Water sample + HFP' and 'Sludge + Water sample + NaAc': (a) residual turbidity and COD; (b) NH_3-N and TN; (c) NO_3-N and NO_2-N; (d) pH and DO; and (e) SVI and MLSS. Three runs were performed and the error bars represented the standard error of the mean of the three runs.

and the running time was 144 h, respectively. HFP was a hybrid-fruit-peel coagulant, and NaAc was sodium acetate, respectively.

3.1.1. Application of HFP in the simulated water

As seen in Figure 2(a), the RT of the effluent in 'S + W' was basically similar to that in 'S + W + NaAc', and both were lower than that in 'S + W + HFP'. Moreover, all of them were lower than 10 NTU, achieving level A discharge standard of 'Discharge standard of pollutants for municipal wastewater treatment Plant' (GB 18918-2002) (MEEPRC 2003). The simulated

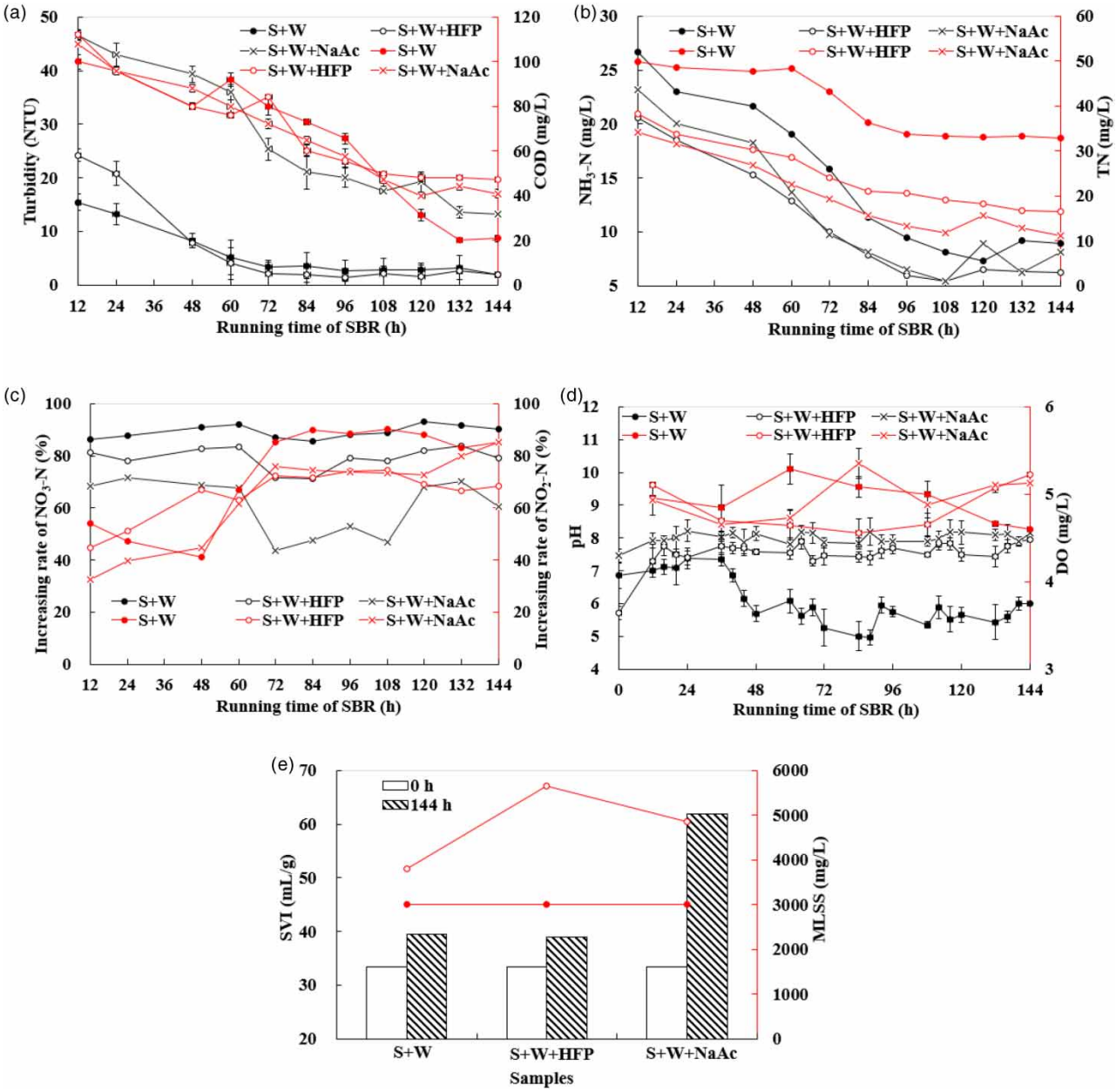

Figure 3 | Comparison of application effect of hybrid-fruit-peel coagulant (HFP) and sodium acetate (NaAc) in the real sewage with sequencing batch reactor (SBR) process between different test systems of 'Sludge + Water sample', 'Sludge + Water sample + HFP' and 'Sludge + Water sample + NaAc': (a) residual turbidity and COD; (b) NH_3-N and TN; (c) NO_3-N and NO_2-N; (d) pH and DO; and (e) SVI and MLSS. Three measurements were carried out for turbidity and COD, pH and DO, and the error bars represented the standard error of the mean of the three measurements.

water was transparent with turbidity lower than 2 NTU, so HFP only gave coagulation action for the sludge, thus leading to a little higher RT in the supernatant. Generally, the coagulation flocs settle easily, so, the high RT of the effluent from 'S + W + HFP' indicated that the coagulation flocs in this situation were floatable, probably conducive to making the flocs contact extensively with pollutants.

As also displayed in Figure 2(a), the COD order of the effluent was as follows: 'S + W + HFP' > 'S + W' > 'S + W + NaAc', with the lowest value of 34, 17.6 and 15.2 mg/L, respectively, consistent with the previous test results, that is, the COD released by HFP was higher than that by NaAc (Yue 2022). Like RT, the COD of the effluent in the three test systems all

achieved the level A discharge standard required by GB 18918-2002. After reaching a certain running time (84 h), the COD of the effluent from 'S + W' and 'S + W + NaAc' basically tended to be stable, compared with a declining process which appeared to be a fluctuating state from 'S + W + HFP'. The fluctuating phenomena and higher COD of the effluent from 'S + W + HFP' probably broadens the adaptability of HFP to water quality changes.

As shown in Figure 2(b), the fluctuating tendency of NH_3-N removal from 'S + W + HFP' was also greater than that from 'S + W + NaAc', but both decreased with the increasing of running time, therefore, it can be considered that the impact of HFP on NH_3-N removal was basically similar to that of NaAc. The removal of TN from 'S + W + HFP' was slightly lower than that from 'S + W + NaAc', but both were down to their lowest value of 15.5 and 12.6 mg/L, respectively, at the end of running time, all far lower than that from 'S + W' (27 mg/L).

As seen in Figure 2(c), the increasing rate of NO_3-N in effluent was basically in the order of 'S + W' > 'S + W + HFP' > 'S + W + NaAc', and the trend of increasing rate of NO_3-N in 'S + W + HFP' was basically consistent with that in 'S + W + NaAc' during the entire running time. This indicated that the accumulation of NO_3-N in 'S + W' was higher, most of the other forms of nitrogen in 'S + W' almost existed in the form of NO_3-N, and 'S + W' gave lower removal of NO_3-N; while HFP gave similar effect on NO_3-N accumulation to NaAc.

Figure 2(c) also showed that the increasing rate of NO_2-N in the effluent was basically in the order of 'S + W + NaAc' > 'S + W' > 'S + W + HFP'. At the beginning of the SBR run, the increasing rate of NO_2-N in 'S + W + NaAc' increased rapidly, compared with the rapid decrease in both 'S + W' and 'S + W + HFP'. And then, the increasing rate of NO_2-N in the three systems basically tended to be stable with the increasing running time, but the time basically reaching stability in 'S + W + HFP' and 'S + W + NaAc' was all 48 h. Although the increasing rate of NO_2-N increased rapidly after 48 h in 'S + W' and then tended to be stable at 72 h or so, the stable value in 'S + W' at 72 h was basically equivalent to that in 'S + W + NaAc' at 72 h, and both were much larger than that in 'S + W + HFP'. This indicated that after a stable run, both 'S + W' and 'S + W + NaAc' probably gave insufficient carbon sources, thus resulting in a rapid accumulation of NO_2-N; however, the carbon sources provided by 'S + W + HFP' was always sufficient, thus leading to a low accumulation of NO_2-N. This also further indicated that HFP has a slow-releasing ability of carbon source.

As shown in Figure 2(d), the DO in 'S + W' decreased rapidly in the later running period due to a rapidly increasing trend of oxygen consumption in the nitrification process, compared with an increasing trend of DO in both 'S + W + HFP' and 'S + W + NaAc', indicating that HFP and NaAc played a similar role as an ECS in the simulated water. As also seen in Figure 2(d), the pH in 'S + W + HFP' and 'S + W + NaAc' was all greater than that in 'S + W', also further indicating that HFP and NaAc basically gave a very similar function of ECS in the simulated water.

As seen in Figure 2(e), compared with the SVI of 33.3 mL/g in 'S + W', the SVI of 'S + W + HFP' and 'S + W + NaAc' all increased, in which the SVI of 'S + W + HFP' was higher than that of 'S + W + NaAc', but both were lower than 60 mL/g, indicating that the SSP of 'S + W + HFP' was lower than that of 'S + W + NaAc', but both were within a relatively suitable range. Meanwhile, the MLSS of 'S + W + HFP' was slightly higher than that of 'S + W + NaAc', because HFP sludge was composed of activated sludge and coagulation flocs or because semi-wrapping/semi-cover of the coagulation flocs on some active microorganisms decreased the activity of sludge to some extent.

3.1.2. Application of HFP in the real sewage

As seen in Figure 3(a), the RT of the effluent from 'S + W' was basically similar to that from 'S + W + HFP', and both were lower than that from 'S + W + NaAc'. Because the coagulation flocs formed by HFP can precipitate easily, the RT in 'S + W + HFP' was lower than 5 NTU, in comparison with more than 20 NTU in 'S + W + NaAc'. So, it can be inferred that HFP gave excellent removal of SS, which was largely different from that in Figure 2(a), because HFP had coagulation behavior for sewage and sludge simultaneously in the real sewage in Figure 3, but only gave coagulation action for sludge in Figure 2 when the simulated water was used as the water sample which was transparent with lower turbidity. This suggested that the coagulation flocs formed from sewage by HFP can precipitate easily, according to the basic aim of wastewater treatment (HFP exert both coagulation and ECS actions in treating wastewaters), but the impact of excellent SSP in 'S + W + HFP' on microbial activity was worth further study. The COD of the effluent from 'S + W + HFP' was basically similar to that from 'S + W + NaAc', with the lowest value of 47.2 and 40.8 mg/L, respectively.

As shown in Figure 3(b), the removal of NH_3-N by HFP was similar to that by NaAc. The removal of TN by HFP was slightly lower than that by NaAc, reducing to the lowest value of 16.5 and 11.1 mg/L, respectively. The removal of NH_3-N and TN from both 'S + W + HFP' and 'S + W + NaAc' were all much higher than that from 'S + W'.

As seen in Figure 3(c), like Figure 2(c), the increasing rate of NO_3-N in the effluent was also basically in the order of 'S + W' > 'S + W + HFP' > 'S + W + NaAc', which was consistent with the simulated water, indicating that the cumulation value of NO_3-N in 'S + W' was also higher in the real sewage. As also seen from Figure 3(c), when basically reaching the running time having relatively stable NO_2-N, the increasing rate of NO_2-N in 'S + W' was greater than that in 'S + W + NaAc' and 'S + W + HFP', and the increasing rate of NO_2-N in 'S + W + HFP' was basically the same as that in 'S + W + NaAc' during the entire running time. Moreover, at the beginning of the run, the increasing rate of NO_2-N in 'S + W + HFP' was greater than that in 'S + W + NaAc', but with the increasing of running time, both almost tended to be stable at 72 h and both almost maintain the same within 36 h after stability. With the further increasing of running time, the increasing rate of NO_2-N in 'S + W + NaAc' was greater than that in 'S + W + HFP'. This indicated that the carbon source provided by NaAc was lower than that by HFP in the later stage of running time, which was the same as the result in Figure 2(c), which also indicated that HFP also gave the ability of slow release carbon source in the real sewage.

As shown in Figure 3(d), the pH and DO developing trends in 'S + W + HFP' and 'S + W + NaAc' were almost the same as that in Figure 2(d), further demonstrating HFP also gave excellent ECS function in the real sewage.

As shown in Figure 3(e), like the simulated water (Figure 2(e)), compared with 'S + W', the SVI of 'S + W + HFP' and 'S + W + NaAc' also all increased, in which the increased value of 'S + W + HFP' was far lower than that of 'S + W + NaAc', but both were also lower than 70 mL/g, suggesting that the SSP of 'S + W + HFP' was far better than that of 'S + W + NaAc', but both were within a relatively suitable range. Meanwhile, the MLSS of HFP was higher than that of NaAc due to the same reason as that in the simulated water (Figure 2(e)).

3.2. Impact of HFP addition on sludge properties

3.2.1. DHA and EPS, and chargeability and size

The simulated water was used as a test water sample in this section.

(1) DHA and EPS

Figure 4 displays the comparison of DHA (Fu *et al.* 2023) and EPS of the sludge in the above test systems ('S', 'S + W', 'S + W + HFP' and 'S + W + NaAc') after SBR run.

DHA is often used as an index to evaluate sludge activity, largely reflecting the ability of microorganisms to metabolize organic matter in the activated sludge. EPS generally refers to all extracellular polymers that are not directly connected with the outer membrane and cell wall materials, mainly deriving from secretions and exfoliated surface materials of cells, cell lysates and adsorbates from the surroundings, mainly including proteins (PN) and polysaccharides (PS).

As seen in Figure 4, the S-PS in 'S', the LB-PS in 'S + W + NaAc' and the TB-PS in 'S + W + HFP' all posed the highest values, respectively, indicating that the sludge in 'S + W + HFP' gave relatively much tighter structure, which is more conducive to the subsequent concentration and dehydration process of the sludge. The S-PN, LB-PN and TB-PN in 'S + W + HFP' all were the highest values, and the PS and PN in 'S + W + HFP' were also the highest, in which the difference of PS in

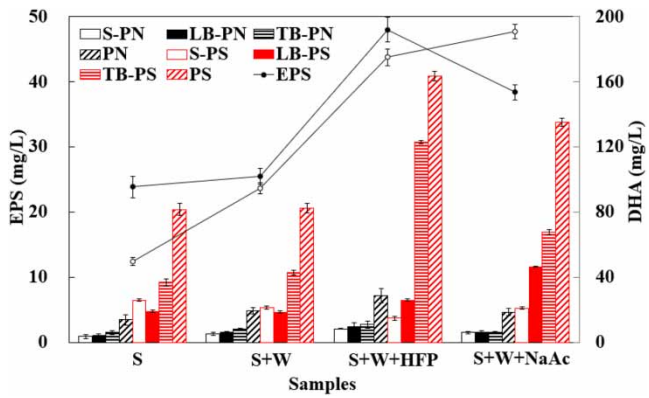

Figure 4 | Comparison of dehydrogenase activity (DHA) and extracellular polymer substance (EPS) of the sludge in the simulated water with sequencing batch reactor (SBR) process between different test systems of 'Sludge', 'Sludge + Water sample', 'Sludge + Water sample + HFP' and 'Sludge + Water sample + NaAc'.

different forms (e.g. S-PS and LB-PS) was greater than that of PN. As well known, PN is the material basis of life, while PS is the energy tissue, so the higher PN in 'S + W + HFP' indicated that HFP promoted more proliferation of microorganisms, which was consistent with the result in Figure 2 and the following Figures 5 and 6. The larger PS in 'S + W + HFP' suggested that HFP contained some cellulose substances which cannot be used as energy, so, the sludge activity decreased to some

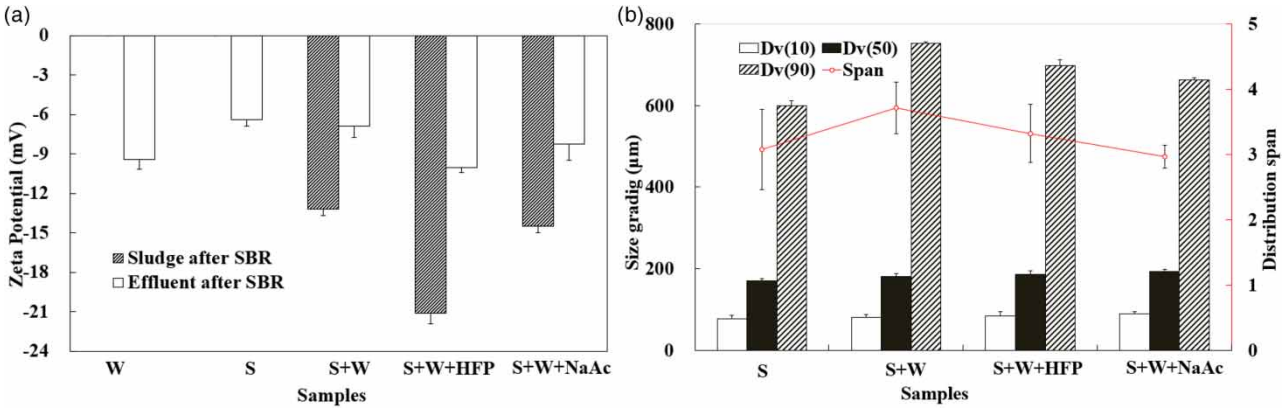

Figure 5 | Comparison of chargeability and size of the sludge in the simulated water with sequencing batch reactor (SBR) process between different test systems of 'Water', 'Sludge', 'Sludge + Water sample', 'Sludge + Water sample + HFP' and 'Sludge + Water sample + NaAc': (a) chargeability and (b) size. HFP, hybrid-fruit-peel coagulant; NaAc, sodium acetate. Three runs were performed, and the error bars represented the standard error of the mean of the three experiments.

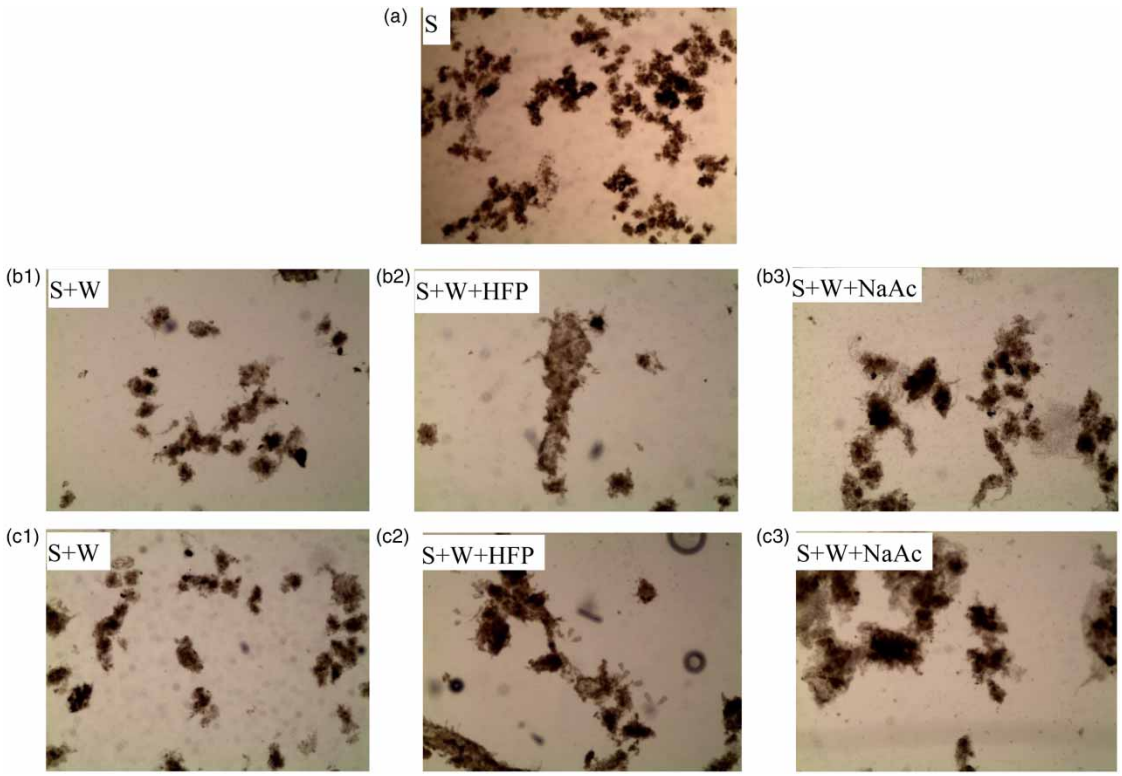

Figure 6 | Comparison of the flocs micrograph changes in the sludge from the real sewage with sequencing batch reactor (SBR) process between different test systems: (a) 'Sludge'; (b) 'Sludge + Water sample', 'Sludge + Water sample + HFP' and'Sludge + Water sample + NaAc' at aeration 3 days; and (c) 'Sludge + Water sample', 'Sludge + Water sample + HFP' and 'Sludge + Water sample + NaAc' at aeration 6 days. HFP, hybrid-fruit-peel coagulant; NaAc, sodium acetate.

extent probably because cellulose substances gave some semi-wrapping for activated sludge, which is also consistent with the result in Figures 2 and 3.

As also seen in Figure 4, the EPS of the sludge in 'S + W + HFP' was significantly higher than that in 'S + W + NaAc', while the DHA in the former was slightly lower than that in the latter, but both were much higher than that in 'S' and 'S + W'. Compared with 'S', the EPS in 'S + W + HFP' and 'S + W + NaAc' increased by 101.2 and 60.8%, and the DHA increased by 252 and 283%, respectively. Moreover, based on the above difference trend of EPS and DHA between HFP and NaAc, it can be concluded that the coagulation behavior of HFP generated more EPS, however, slightly decreased the sludge activity, which was also further consistent with the results in Figure 2.

Figure 4(a) also showed the DHA difference between 'S + W + HFP' and 'S + W + NaAc' was relatively smaller, so HFP can still be used as a high-quality ECS, also further demonstrating that HFP has the potentiality of becoming a slow-releasing carbon source, which was consistent with the results of Figures 2(c) and 3(c).

(2) Chargeability and size

Figure 5 shows the comparison of the chargeability of effluent and surplus sludge from SBR systems (Figure 5(a)) and the size of the sludge (Figure 5(b)) between different test systems of 'S + W', 'S + W + HFP' and 'S + W + NaAc' after SBR process.

As seen from Figure 5(a), the sludge in 'S + W + HFP' posed the highest negative charge and gave much higher negative charge than that in 'S' and 'S + W + NaAc', while the negative charge carried by the sludge in 'S + W + NaAc' was slightly higher than that in 'S + W', indicating that the sludge in 'S + W + HFP' gave the highest activity, and the sludge activity in 'S + W + NaAc' was slightly higher than that in 'S'. For the effluent, except for 'S', there is almost little difference in the negative charges in the other test systems, demonstrating that HFP or NaAc mainly had some impact on the charge carried by the sludge, which is also the basic purpose of adding ECS.

Dv in Figure 5(b) refers to the cumulative particle size distribution of volume. For example, Dv(50) represents the particle size when the percentage of cumulative particle size distribution reached 50% in the samples. As shown in Figure 5(b), compared with 'S', Dv(10), Dv(50) and Dv(90) of the sludge in 'S + W + HFP' and 'S + W + NaAc' all increased slightly, increased by 8, 15 and 99 μm in 'S + W + HFP', respectively, compared with 13.1, 23 and 63 μm in 'S + W + NaAc'. This indicated that the sludge size all increased after adding ECS, but there appeared many structures of larger size sludge in 'S + W + HFP', probably because the coagulation behavior of HFP generated some flocs having larger sizes.

3.2.2. Micrographs and biofacies

Figure 6 shows the comparison of micrographs between the acclimation sludge (Figure 6(a)) and the surplus sludge in 'S + W', 'S + W + HFP' and 'S + W + NaAc' at aeration time of 3 days (Figure 6(b)) and 6 days (Figure 6(c)), respectively. Figure 7 shows the comparison of biofacies between the acclimation sludge (Figure 7(a)) and the surplus sludge in 'S + W', 'S + W + HFP' and 'S + W + NaAc' at aeration time of 3 days (Figure 7(b)) and 6 days (Figure 7(c)), respectively.

As shown in Figure 6(a), the acclimation sludge flocs in scattered distribution gave a clear edge of the interface. The floc distribution became looser and less with the increasing aeration time (e.g. from 0 to 3 days, and then to 6 days), but the edge of their interface was still clearer with still relatively even and small size.

As seen in Figure 6(b) and 6(c), the sizes of the sludge flocs in 'S + W + HFP' and 'S + W + NaAc' increased obviously after aeration for 3 days, and some semi-transparent thin cotton-like substances appeared at the edge of the interface between flocs, which was assumed to be transparent mucous substances generated by microorganisms. The amount of mucous substances in 'S + W + HFP' was obviously more than those in 'S + W + NaAc', and the adhesive degree between flocs was also significantly higher than that in 'S + W + NaAc '. In addition, the size of the sludge flocs in 'S + W + HFP' was also larger than that in 'S + W + NaAc', further indicating HFP coagulation action formed some flocs having a larger size. When the aeration time was from 3 to 6 days, the size of the sludge in 'S + W + HFP' and 'S + W + NaAc' became significantly larger, the semi-transparent mucous substances also increased obviously and the connection between the flocs became closer.

In addition, as also seen in Figure 6, the semi-transparent mucous substances at the edge of sludge in 'S + W + HFP' was not obvious, because the coagulation flocs and microbial flocs may be in an overlapped or semi-wrapped situation to some extent, thus covering the mucous substances. Besides, the sludge flocs in 'S + W + HFP' gave larger size and greater extensibility, in comparison with that in 'S + W + NaAc' (much flocs appeared to be in clustered state in 'S + W + NaAc'), indicating 'S + W + HFP' gave larger surface area and amount of sludge flocs which will be conducive to contact directly to pollutants and remove pollutants.

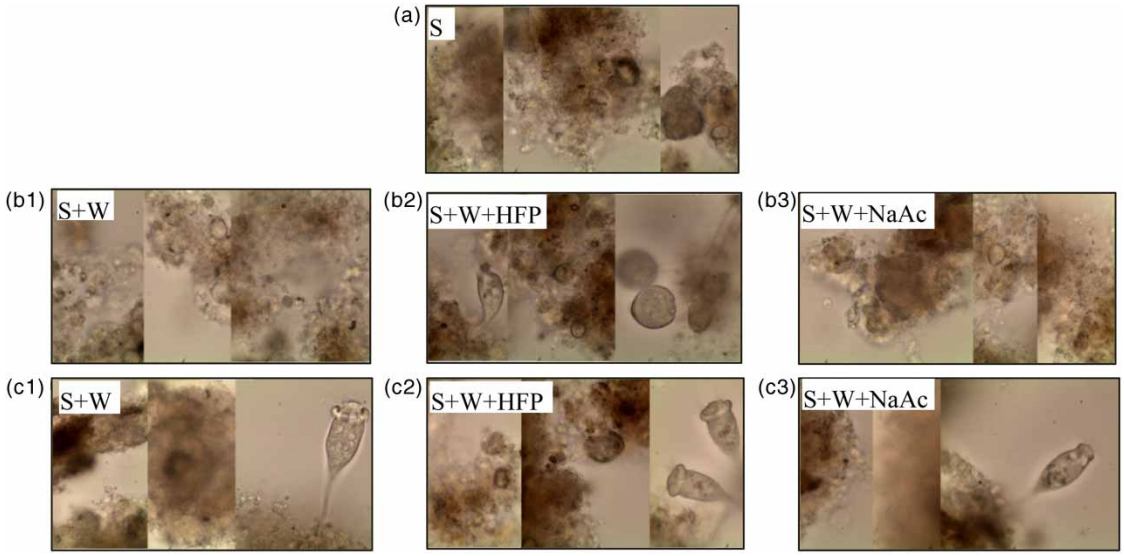

Figure 7 | Comparison of the flocs biofacies collected from the sludge after adding hybrid-fruit-peel coagulant (HFP) and sodium acetate (NaAc) as ECS to the real sewage with sequencing batch reactor (SBR) process between different test systems: (a) 'Sludge'; (b) 'Sludge + Water sample', 'Sludge + Water sample + HFP' and'Sludge + Water sample + NaAc' at aeration 3 days; and (c) 'Sludge + Water sample', 'Sludge + Water sample + HFP' and 'Sludge + Water sample + NaAc' at aeration 6 days. HFP, hybrid-fruit-peel coagulant; NaAc, sodium acetate.

To sum up, the edge interface of the acclimation sludge flocs appeared to be clear and in scattered distribution, whose size was relatively even and small. After the addition of HFP and NaAc, the sizes of the flocs were increased obviously. Many flocs after adding NaAc appeared to be clustered type and were not conducive to the contact and removal of pollutants, while the flocs of HFP had larger surface areas and were conducive to directly contact pollutants and remove pollutants.

By observation under magnification 400 times (Figure 7), the sludge in this experiment was mainly composed of spherical and filamentous bacteria. The species and number of microorganisms also increased significantly after the addition of HFP and NaAc, generating more protozoa (such as nematode, vorticella, wheel animalcule, etc.) in 'S + W + HFP' than that in 'S + W + NaAc' and 'S + W', suggesting that the effluent of 'S + W + HFP' gave better qualities. In addition, these organisms were very active under the microscope.

From the application results of HFP in the real sewage, NaAc only prompted a certain amount of sludge proliferation, but HFP coagulation action promoted the condensation of suspended flocs, producing much larger size floc structures, further promoting a great reduction of turbidity in the supernatant. Therefore, as an ECS, NaAc may not be conducive to SS removal, thus resulting in some increasing difficulty of advanced treatment, while HFP is more conducive to SS removal.

So, HFP can be used as an excellent ECS for low carbon source wastewater.

4. CONCLUSIONS

HFP gives a similar ECS action to NaAc, and can be used as a high-quality ECS for treating low carbon source wastewaters and has the ability to slow-release carbon sources.

As an additional carbon source for the simulated and real wastewater with the SBR process, HFP almost had similar nitrogen removal (NH_3-N or TN), and the developing trend of both DO and pH to NaAc. For the real sewage, HFP gave higher turbidity (i.e. SS) removal than NaAc. For the above test water samples, the accumulation trend of NO_2-N rise in 'S + W + HFP' was basically the same as that in 'S + W + NaAc', but 'S + W + NaAc' gave lower NO_2-N rise than 'S + W + HFP' at the late stage of the running stage. The PN and PS of the sludge after HFP addition were higher than that of NaAc (i.e. HFP generated more PS and promoted more proliferation of microorganisms), but its DHA was slightly decreased compared with that of NaAc (i.e. probably decreasing the activity of HFP sludge to some extent). Compared with NaAc, HFP produced more sludge flocs having larger size, much closer connection and greater extensibility, thus was conducive to removing pollutants. The sludge in the 'S + T + HFP' system was mainly composed of spherical and filamentous bacteria with more protozoa (such as nematode, vorticella, wheel animalcule, etc.), giving better effluent qualities.

In the near future, some research on the impact of HFP coagulation behavior on both microbial types and subsequent wastewater treatment, and on optimization and improvement of preparation scheme of HFP based on the qualities of various wastewaters will be conducted further.

ACKNOWLEDGEMENTS

The authors acknowledge the financial support of the Shandong Province enterprise technology innovation project from the Department of Industry and Information Technology of Shandong Province (202150100867), Research Center of Shuifa Technology Group, University of Jinan (202012 and w2021125). The authors also thank the editor and the anonymous reviewers for their valuable comments to improve the quality of this paper.

DATA AVAILABILITY STATEMENT

All relevant data are included in the paper or its Supplementary Information.

CONFLICT OF INTEREST

The authors declare there is no conflict.

REFERENCES

Awual, M. R. 2019 Efficient phosphate removal from water for controlling eutrophication using novel composite adsorbent. *Journal of Cleaner Production* **228**, 1311–1319.

Barros, A. R. M., Carvalho, C. A., Firmino, P. I. M. & Santos, A. B. S. 2021 Effect of calcium addition to aerobic granular sludge systems under high (conventional SBR) and low (simultaneous fill/draw SBR) selection pressure. *Environmental Research* **194**, 110639.

Bi, Z. H., Zhang, Q., Xu, X. J., Yuan, Y., Ren, N. Q., Lee, D. J. & Chen, C. 2022 Perspective on inorganic electron donor-mediated biological denitrification process for low C/N wastewaters. *Bioresource Technology* **363**, 127890.

Chang, M. D., Liang, B. R., Zhang, K., Wang, Y. Z., Jin, D. T., Zhang, Q. J., Hao, L. Y. & Zhu, T. 2021 Simultaneous shortcut nitrification and denitrification in a hybrid membrane aerated biofilms reactor (H-MBfR) for nitrogen removal from low COD/N wastewater. *Water Research* **211**, 118027.

Cherchi, C., Onnis-Hayden, A., El-Shawabkeh, I. & Gu, A. Z. 2009 Implication of using different carbon sources for denitrification in wastewater treatments. *Water Environment Research* **81**, 788–799.

Feng, Z. T., Ma, X., Sun, Y. J., Zhou, J. M., Liao, Z. G., He, Z. C., Ding, F. & Zhang, Q. Q. 2023 Promotion of nitrogen removal in a denitrification process elevated by zero-valent iron under low carbon-to-nitrogen ratio. *Bioresource Technology* **386**, 129566.

Fu, Y. & Meng, X. J. 2021 Corresponding relationship between microorganism propagation and coagulation behavior of a hybrid fruit-peel coagulant. *Desalination and Water Treatment* **216**, 326–337.

Fu, Y., Meng, X. J., Lu, N. N., Jian, H. L. & Di, Y. 2019 Characteristics changes in banana peel coagulant during storage process. *International Journal of Environmental Science and Technology* **16**, 7747–7756.

Fu, X. R., Hou, R. R., Yang, P., Qian, S. T., Feng, Z. Q., Chen, Z. B., Wang, F., Yuan, R. F., Chen, H. L. & Zhou, B. H. 2022 Application of external carbon source in heterotrophic denitrification of domestic sewage: A review. *Science of the Total Environment* **817**, 153061.

Fu, Y., Yue, Q. H., Luo, S. Y., Tian, X., Zheng, J. W. & Yang, Y. T. 2023 Two kinds of behavior of fruit peel coagulant in treating low carbon source wastewaters. *Environmental Engineering Research* **28** (4), 220223.

Gu, J., Zhang, M., Wang, S. & Liu, Y. 2019 Integrated upflow anaerobic fixed-bed and single-stage step-feed process for mainstream deammonification: A step further towards sustainable municipal wastewater reclamation. *Science of the Total Environment* **678**, 559–564.

Hameed, B. H., Mahmoud, D. K. & Ahmad, A. L. 2008 Sorption of basic dye from aqueous solution by pomelo (*Citrus grandis*) peel in a batch system. *Colloids and Surfaces* **316**, 78–84.

Hang, Q., Wang, H., Chu, Z., Ye, B., Li, C. & Hou, Z. 2016 Application of plant carbon source for denitrification by constructed wetland and bioreactor: Review of recent development. *Environmental Science and Pollution Research* **23**, 8260–8274.

Hu, R. T., Zheng, X. L., Zheng, T. Y., Xin, J., Wang, H. & Sun, Q. G. 2019 Effects of carbon availability in a woody carbon source on its nitrate removal behavior in solid-phase denitrification. *Journal of Environmental Management* **246**, 832–839.

Hu, H. D., Ma, S. J., Zhang, X. X. & Ren, H. Q. 2020 Characteristics of dissolved organic nitrogen in effluent from a biological nitrogen removal process using sludge alkaline fermentation liquid as an external carbon source. *Water Research* **176**, 115741.

Huang, X. W. & Lee, P. H. 2020 Shortcut nitrification/denitrification through limited-oxygen supply with two extreme COD/N-and-ammonia active landfill leachates. *Chemical Engineering Journal* **404**, 126511.

Jian, H. L. 2019 *Preparation and Performance of a Hybrid Fruit-Peel Coagulant. Master degree Thesis*, University of Jinan, China. (In Chinese).

Jiang, L., Liu, J. Y., Zuo, K., Zou, L. P., Li, Y. Y., Qian, G. G. & Xu, Z. P. 2018 Performance of layered double hydroxides intercalated with acetate as biodenitrification carbon source: The effects of metal ions and particle size. *Bioresource Technology* **259**, 99–103.

Kim, S. 2022 Blending of waste biomass for cost-effective chitosan-based biosorbents for removal of reactive dye from aqueous solution. *Environmental Engineering Research* **27**, 210457.

Li, Y. Y., Huang, X. W. & Li, X. Y. 2021 Using anammox biofilms for rapid start-up of partial nitritation-anammox in integrated fixed-film activated sludge for autotrophic nitrogen removal. *Science of the Total Environment* **791**, 148314.

Li, P. L., Xiong, S. J., Wang, Q. C., Xue, C. Y., Xiao, P. & Qian, G. S. 2023 Enhancement strategies of aerobic denitrification for efficient nitrogen removal from low carbon-to-nitrogen ratio shale oil wastewater. *Bioresource Technology* **387**, 129663.

Lu, N. N. 2017 *Preparation of Fruit-Skin Coagulant and its Coagulation Performance in Water Treatment*. *Master degree Thesis*, University of Jinan, China. (In Chinese).

Ma, B., Xu, X. X., Gao, M. H., Wei, Y. & Peng, Y. Z. 2020 Advanced nitrogen removal characteristics of low carbon source municipal wastewater treatment via partial-denitrification coupled with ANAMMOX. *Environmental Science* **41**, 1377–1383. (In Chinese).

Mahmoud, A., Hamza, R. A. & Elbeshbishy, E. 2022 Enhancement of denitrification efficiency using municipal and industrial waste fermentation liquids as external carbon sources. *Science of the Total Environment* **816**, 151578.

Ministry of Ecology and Environment of the People's Republic of China (MEEPRC). 2003 Discharge standard of pollutants for municipal wastewater treatment plant (GB 18918-2002). 2003-07-01. Available from: https://www.mee.gov.cn/ywgz/fgbz/bz/bzwb/shjbh/swrwpfbz/200307/t20030701_66529.shtml. (In Chinese).

Narancic, T., Cerrone, F., Beagan, N. & O'Connor, K. E. 2020 Recent advances in bioplastics: Application and biodegradation. *Polymers* **12**, 920.

Pelaz, L., Gomez, A., Letona, A., Garralon, G. & Fdz-Polanco, M. 2018 Nitrogen removal in domestic wastewater. Effect of nitrate recycling and COD/N ratio. *Chemosphere* **212**, 8–14.

Qi, S. S., Wang, Y. L., Chu, X. Q., Wang, W. & Hu, Z. H. 2020 Food waste fermentation for carbon source production and denitrification in sequencing batch reactors. *Journal of Cleaner Production* **253**, 119934.

Shalini, S. S. & Joseph, K. 2018 Combined SHARON and ANAMMOX processes for ammoniacal nitrogen stabilisation in landfill bioreactors. *Bioresource Technology* **250**, 723–732.

Sun, Y. L. 2020 Connotation and way of quality and efficiency improvement of municipal wastewater treatment. *China Water & Wastewater* **36**, 1–6. (In Chinese).

Sun, P. Z., Wu, J. Q. & Kang, L. M. 2020 Effect of influence modes and recirculation point position on nitrogen and phosphorus removal by a multi-stage biological contact oxidation process. *Environmental Engineering* **38**, 54–59, 195. (In Chinese).

Tao, C., Parker, W. & Bérubé, P. 2022 Evaluation of the impact of SBR operating temperature and filtration temperature on fouling of membranes used for tertiary treatment. *Separation and Purification Technology* **294**, 121194.

Torresi, E., Escola, C. M., Polesel, F., Plosz, B. G., Christensson, M. & Bester, K. 2017 Impact of external carbon dose on the removal of micropollutants using methanol and ethanol in post-denitrifying moving bed biofilm reactors. *Water Research* **108**, 95–105.

Wang, S. Y., Zhu, G. B., Li, Y. F., Wang, X. X., Zhou, J. M. & Peng, Y. Z. 2019 Robustness of anammox granular sludge treating low-strength sewage under various shock loadings: Microbial mechanism and little N_2O emission. *Journal of Environmental Sciences* **86**, 141–153.

Xiong, R., Yu, X., Yu, L., Peng, Z., Cheng, L. & Fan, P. 2019 Biological denitrification using polycaprolactone-peanut shell as slow-release carbon source treating drainage of municipal WWTP. *Chemosphere* **235**, 434–439.

Xiong, R., Yu, X. X., Zhang, Y. G., Peng, Z. X., Yu, L. J., Cheng, L. L. & Li, T. M. 2020 Comparison of agricultural wastes and synthetic macromolecules as solid carbon source in treating low carbon nitrogen wastewater. *Science of the Total Environment* **739**, 139885.

Yu, C. Q., Huang, X., Chen, H., Godfray, H. C. J., Wrigh, J. S., Hall, J. W., Gong, P., Ni, S. Q., Qiao, S. C., Huang, G. R., Xiao, Y. C., Zhang, J., Feng, Z., Ju, X. T., Ciais, P., Stenseth, N. C., Hessen, D. O., Sun, Z. L., Yu, L., Cai, W. J., Fu, H. H., Huang, X. M., Zhang, C., Liu, H. B. & Taylor, J. 2019a Managing nitrogen to restore water quality in China. *Nature* **567**, 516–520.

Yu, G. L., Peng, H. Y., Fu, Y. J., Yan, X. J., Dua, C. Y. & Chen, H. 2019b Enhanced nitrogen removal of low C/N wastewater in constructed wetlands with co-immobilizing solid carbon source and denitrifying bacteria. *Bioresource Technology* **280**, 337–344.

Yue, Q. H. 2022 *Effect of Fruit Peel Coagulant on Activated Sludge Performance in Wastewater of low Carbon Source*. *Master degree Thesis*, University of Jinan, China. (In Chinese).

Zeeshan, M., Hussain, F., Ahmad, W. & Khan, K. 2020 Impact of biochar particle sizes on the bioaccumulation of the heavy metals and their target hazard assessment. *Environmental Engineering Science* **27**, 614–622.

Zhang, Y. Y., Wei, W. & Zhu, S. G. 2021 Research progress on denitrification of low carbon source municipal wastewater. *Journal of Anhui Jianzhu University* **29**, 58–63. (In Chinese).

Zhang, K. Q., Fang, Q., Xie, Y. H., Chen, Y. J., Wei, T. & Xiao, Y. Y. 2022 The synthesis of polyhydroxyalkanoates from low carbon wastewater under anaerobic-microaerobic process: Effects of pH and nitrogen and phosphorus limitation. *Environmental Engineering Research* **27**, 210467.

Zhao, J. M., He, Q. C., Chen, N., Peng, T. & Feng, C. P. 2020 Denitrification behavior in a woodchip-packed bioreactor with gradient filling for nitrate-contaminated water treatment. *Biochemical Engineering Journal* **154**, 107454.

Zhong, F., Huang, S., Wu, J., Cheng, S. & Deng, Z. 2019 The use of microalgal biomass as a carbon source for nitrate removal in horizontal subsurface flow constructed wetlands. *Ecological Engineering* **127**, 263–267.

Zhou, B., Duan, J., Xue, L., Zhang, J. & Yang, L. 2019 Effect of plant-based carbon source supplements on denitrification of synthetic wastewater: Focus on the microbiology. *Environmental Science and Pollution Research* **26**, 24683–24694.

First received 19 August 2023; accepted in revised form 18 November 2023. Available online 22 December 2023